Materiales de Construcción
Vol. 73, Issue 352, October-December 2023, e327
ISSN-L: 0465-2746
https://doi.org/10.3989/mc.2023.351623

Exploring the impact of graphene oxide on mechanical and durability properties of mortars incorporating demolition waste: micro and nano-pore structure effects

C. Chacón-Bonet [a], H. Cifuentes [b], Y. Luna [a], J.D. Ríos [c], M.P. Ariza [b], C. Leiva [a] ✉

a. Department of Chemical and Environmental Engineering. University of Seville, (Seville, Spain)
b. Department of Continuum Mechanics and Structural Analysis. University of Seville. Universidad de Sevilla, (Seville, Spain)
c. Department of Mechanical, Energy and Materials Engineering. University of Extremadura, (Badajoz, Spain)
✉: cleiva@us.es

Received 28 March 2023
Accepted 14 July 2023
Available on line 8 November 2023

ABSTRACT: In this study is explored the use of construction and demolition waste as fine aggregate in mortars. The addition of nano-graphene oxide (0.1%wt) has also been evaluated. Tests were conducted to determine their density, humidity content, water absorption capacity and open void porosity (using water absorption) and the micro and nano-porosity using Hg intrusion and N_2 absorption techniques, as well as their flexural and compressive strength and resistance to acid attacks. The mechanical properties of mortars manufactured with standard sand were better (30%) than made with waste aggregate. Mortars with both aggregates can be classified as M20. Nano-Graphene oxide acts as a filler, reducing the volume of macro and micro pores, thereby increasing the mechanical performance, especially when recycled aggregates are used (30% the flexural strength for recycled aggregates and 4% for standard sand). The addition of nano-graphene oxide reduces the transmission channels of acid within mortar.

KEY WORDS: Construction and demolition waste aggregate; Nano-graphene oxide; Mechanical properties; Porosity, Acid attack.

Citation/Citar como: Chacón-Bonet, C.; Cifuentes, H.; Luna, J.; Ríos, D.; Ariza, M.P.; Leiva, C. (2023) Exploring the impact of graphene oxide on mechanical and durability properties of mortars incorporating demolition waste: micro and nano-pore structure effects. Mater. Construcc. 73 (352), e327. https://doi.org/10.3989/mc.2023.351623.

RESUMEN: *Explorando el impacto del óxido de grafeno en las propiedades mecánicas y de durabilidad de los morteros que incorporan residuos de demolición: efectos en la estructura de micro y nano-poros*. Este estudio explora el uso de residuos de construcción y demolición como árido fino en morteros. Se ha evaluado la adición de nano-óxido de grafeno (0.1%p). Se ha analizado la porosidad abierta usando absorción de agua, micro-porosidad con intrusión de Hg y nano-porosidad por absorción de N_2, así como su resistencia a la flexión, compresión y resistencia al ataque ácido. Las propiedades mecánicas con arena estándar fueron mejores (30%) que, con árido reciclado, aunque los dos morteros pueden ser clasificados como M20. El volumen de macro y micro-poros disminuyó con nano-oxido de grafeno, lo que aumentó las propiedades mecánicas, especialmente cuando se utilizan agregados reciclados (30 % de la resistencia a la flexión para áridos reciclados y 4 % para áridos estándar). La adición de nano-oxido grafeno reduce los canales de transmisión de ácido dentro del mortero aumentando la resistencia a compresión tras el ataque ácido.

PALABRAS CLAVE: Residuos de construcción y demolición; Nano-óxido de grafeno; Propiedades mecánicas; Porosidad; Ataque ácido.

1. INTRODUCTION

The rapid increase in urbanization and industrialization is leading to a growing trend in construction and demolition waste (CDW). The production of construction and demolition waste has increased to 3.5 billion tons/year, which is a threat to the environment (1). The large amounts of waste generated by the construction sector negatively affect the environment due to the lack of appropriate disposal sites and the use of inadequate disposal methods (2). In the last 10 years, only in Europe, construction activity generated around 827 million tons of CDW on average per year and only 50% of them were reclaimed (3).

In Spain, waste management is regulated by Directive (EU) 2018/851 (4) amending Directive 2008/98/EC on waste (5), which includes the definition of CDW as "waste generated by construction and demolition activities" (6). The Spanish State Waste Management Framework Plan (PEMAR) 2016-2022 establishes a minimum percentage of non-hazardous CDW destined for preparation for reuse, recycling, and other recovery operations (excluding clean soil and stones) and a maximum percentage of non-hazardous CDW disposal in landfills. The values are shown on Table 1 (7).

Construction and demolition waste results mainly from the demolition of buildings or the rejection of building materials from new construction sites and home renovations. A considerable part of this waste is sent to landfills, with a negative visual, landscape and environmental impact because of the disposal of materials that could be recycled with proper treatment (8).

These problems provide an incentive to develop recycling alternatives and to exploit their potential as secondary materials. Research and technology for recycling construction waste makes it possible not only to conserve many aggregate natural resources but also to reduce construction waste, which is consistent with the sustainability requirements of the construction industry (1, 9, 10).

Recycled concrete aggregates exhibit a certain heterogeneity in their properties due to the different characteristics of the materials that are sent to recycling plants, crushing systems and impurities. To ensure that CDWs are inert or non-hazardous materials, they undergo a selection, cleaning, and separation process, after which they are subjected to treatment if necessary. The recycled aggregate obtained from the original concrete after the crushing process is a mixture of coarse aggregate (≥ 4 mm) and fine aggregate (< 4 mm) (11).

Recycled aggregate as a replacement for standard sand in cementitious composites has already been explored in various studies (12-14). Research has shown that recycled sand (RS) has more porous structures and higher water adsorption than standard sand (SS). The bond between RS and the cement matrix has been found to be weaker than in SS cement composites. These results have revealed that the use of RS to replace SS reduces the mechanical properties of cementitious composites.

In Spain, aggregates for mortars must satisfy the following standards:

- EN 13139:2003 "Aggregates for mortars" (15).
- prEN 12620: 2002 Aggregates for concrete (16).
- EN 13055-1: 2003 Lightweight aggregates - Part 1: Lightweight aggregates for concrete, mortar and grout (17).
- prEN 13242:2017 Aggregates for bituminous mixtures and surface treatments for roads, airfields and other trafficked areas (18).

To improve the mechanical performance of cement composites with recycled aggregates, various reinforcements such as graphene oxide (GO) have been used in the concrete industry (19-21). Graphene oxide is a derivative of graphene that can be described as a layer of graphene with functional oxygen groups grafted (22). These oxygen-containing groups contribute to make GO sheets hydrophilic and highly dispersible in water (1). The main approach used to manufacture cement-GO composites simply involves ultrasonication of GO dispersion in water, prior to mixing with cement. GO is a material with a planar structure and excellent mechanical properties that has the potential to improve the hardness of calcium silicate hydrate (C-S-H). This material can significantly improve the tenacity and strength of concrete and other cement-based materials (23).

Table 1. Spanish State Waste Management Framework Plan (PEMAR) 2016-2022.

Minimum % of non-hazardous CDW destined for preparation for reuse, recycling, and other recovery operations		
60% in 2016	65% in 2018	70% in 2020
Maximum % of non-hazardous CDW disposal in landfills		
40% in 2016	35% in 2018	30% in 2020

GO in cementitious materials began to appear in the literature in 2011. Some of the first studies were conducted by Lv et al. (24-25). These authors suggested that GO was a great reinforcement for cement products that was able, for example, to enhance flexural strength by more than 60%. There is currently a controversy between the results reported by different researchers on GO-reinforced cement products because other studies (26-27) have shown no improvements or even disadvantages (28-30). It could be thought that discrepancies between results are due to the existence of significant differences between studies. Considering previous studies, two important factors can be observed to explain this controversy: a) the different particle size of GO after the necessary ultrasonication and b) the different porosity of the matrix to which GO is added (which depends on the water/cement ratio and the particle size of materials).

This study had a dual objective: to explore the possibility of recycling construction and demolition waste by replacing all the standard sand used in mortar composites, and to analyze how the addition of GO affects mortars with both types of aggregates. The implementation of the results of this study will promote more sustainable construction practices, which will contribute to reducing the amount of construction and demolition waste that ends up in landfills as well as the costs in the construction industry will be reduced. On the other hand, mortars with nano-graphene oxide addition could exhibit increased durability, especially in terms of resistance to moisture ingress, chemical attack, and carbonation, as well as reduction of porosity which could lead to higher strength. This enhanced durability would contribute to longer-lasting structures, reducing maintenance and repair costs over time.

2. MATERIALS AND METHODS

2.1. Materials

For the production of the different compositions explored in this study, several components were used: Portland cement (CEM II/B-L 32.5 N) conforming to EN 197-1 (31); standard sand (i.e., natural river sand) conforming to EN 196-1 (31); and sand from CDW obtained from the ALCOREC plant in San Jose de la Rinconada (Seville, Spain). Both sands were previously sieved to obtain a maximum particle size of 1.25 mm.

Figure 1 shows the comparison between standard sand and recycled sand as received (without previous sieve). At first sight, it can be seen that demolition waste has larger particles than standard sand. The colour is different, with recycled sand having a cementitious colour and standard sand having a more intense yellowish colour.

2.2. Preparation of mortars

The dosage of each component was conducted by weighing them according to the established ratio shown on Table 2.

The water/cement ratio is higher in mortars with recycled aggregates, due to their low specific gravity. CDW absorbs water during the mixing process, and a high water/cement ratio is necessary to obtain a homogeneous mix (32).

Cement and sand (standard or recycled) were weighed and mixed for 30 seconds in a laboratory mixer. Next, water was added and mixed with the solids for 2 minutes, until a homogeneous paste was obtained. When

Figure 1. Standard sand (left) and demolition and construction waste (right) as fine aggregate.

Table 2. Compositions of mixtures.

Mix design / Material		Cement (kg)	Standard sand (kg)	Recycled sand (kg)	Water (L)	Graphene oxide (kg)
I	**SS -W/PC=0.37**	333.3	999.9	-	123.3	-
II	**SS -W/PC=0.45**				150.0	
III	**SS -W/PC=0.5**				166.7	
IV	**SS – W/PC=0.37 – GO**				123.3	0.10
V	**RS -W/PC=0.5**		-	999.9	166.7	-
VI	**RS -W/PC=0.6**				200.0	
VII	**RS -W/PC=0.6 – GO**					0.10

GO was added, the required GO at a concentration of 4 g/L (Graphenea) was previously stirred for 24 hours and sonicated for 15 minutes. All GO solutions had the same concentration during sonication. The sonicated solution was mixed with clean water (i.e., without GO) and then added to the solids. The dose of GO (0.0075% of solid content) was chosen according to a previous study (26).

The material was left in the mould for 24 hours so that it was hard enough for demoulding. After demoulding, the mortars were placed in water for 14 days to cure. At the end of this period, they were removed from the water and exposed to air for 13 days. After 28 days, they were ready for exploring their physical and mechanical properties.

2.3. Leaching study

Given that waste is used in mortars, a leaching test was necessary. According to European standards, construction materials should not emit hazardous substances, but, for example, in Spain, no national tests or limits are specified to evaluate the leaching properties of construction materials containing waste. This study was conducted in accordance with the EN-12457 (33) waste characterization standard. It is a conformity test for the leaching of granular waste and sludge including a one-stage batch test with a liquid-solid ratio of 10 l/kg for waste with a particle size of less than 10 mm. This test is the most common leaching test in Europe to classify wastes, and some countries, such as Italy (34), use the results of this test to determine whether a residue can be used in building materials when compared to certain reference values. This test is a protocol used to accelerate the release of chemical species contained in a material in order to characterize its potential to be mobilized into the environment. The pollutants of greatest interest that can be mobilized by weathering and leaching due to rainfall are heavy metals, due to their high toxicity at low concentrations. Analysis in leachates was carried out through Inductively Coupled Plasma technique.

2.4. Physical properties

2.4.1. Density

Density is one of the main properties of construction products, as it affects other properties such as compressive and flexural strength. The density of the different mortars was determined by their weight and volume dimensions. The density was carried out on 15 cylindrical samples of 33 mm of diameter and 40 mm of heigh.

2.4.2. Humidity content

The water content of the mortars after 28 days is obtained from the change in weight observed in the samples at room temperature when weighed before introducing them into the oven and after curing in an oven at 105 ˚C until the weight of the samples is constant (35). The humidity content of each mortar was determined using the following Equation [1]:

$$H\ (\%) = \frac{W_o - W_d}{W_d} \cdot 100 \qquad [1]$$

where H (%) is the humidity content, W_o is the initial weight and W_d is the dried weight. The test was carried out on 3 cylindrical samples of 33 mm of diameter and 40 mm of heigh.

2.4.3. Water absorption capacity

The water absorbed by the materials was obtained from the weight change produced in the samples

during a period of two hours immersed in a water bath (35). After this time, they reached their saturation weight. Water absorption was obtained with the following Equation [2]:

$$A\ (\%) = \frac{W_s - W_d}{W_d} \cdot 100 \qquad [2]$$

where: A (%) is the Water absorption capacity, W_s is Saturation weight and W_d is the dried weight. The test was carried out on 3 cylindrical samples of 33 mm of diameter and 40 mm of heigh.

2.4.4. Open void porosity ratio

To determine the open void ratio (36), the samples were dried in the oven at 105 ± 5 ºC. Next, they were weighed (W_d) and left under water in a vacuum vessel completely submerged until saturation was reached. After 24 hours, they were removed and reweighed (W_S). The proportion of open voids was calculated with the following Equation [3]:

$$VR\ (\%) = \frac{V_w}{V} \cdot 100 \qquad [3]$$

where: V is the Total volume of the sample and V_w is Volume of the sample occupied by water, which can be expressed as (Equation [4]):

$$V_w = \frac{W_S - W_d}{\rho_w} \qquad [4]$$

where ρ_w is the Density of water. The test was carried out on 3 cylindrical samples of 33 mm of diameter and 40 mm of heigh.

2.4.5. Pore size distribution

A pore size analysis was performed. Micromeritics Autopore IV mercury intrusion porosimeter was employed. The quantifiable pore size was in the range of 0.007 to 150 mm. The samples had to be dried in an oven at 105 °C until a constant mass was achieved because they were in the form of pellets that were around 5 mm in size. Gas adsorption measurements were performed at -196 ºC using N_2 in a Micromeritics ASAP 2020 analyzer.

Scanning electron microscopy (SEM) was performed with a JEOL JSM-5600 instrument. All of the samples were bonded to a thin coating of a quick-drying epoxy glue on an aluminum specimen stub, and then gold was sputter coated to a thickness of 10 nm to prevent charging effects.

2.5. Mechanical properties

Flexural strength was determined according to ASTM C-348-02 (37). Three different parallelepipeds 160 × 40 × 40 mm were used and tested at a loading rate of 15 mm/min. The equipment used to calculate flexural strength was the same as that used for the compression test: the Suzpecar machine, model MEM102/50 t.

Compressive strength was measured at the age of 28 days following the procedure given in EN 196-1 (38). The two pieces of each sample after the flexural test (6 samples) were subjected to compressive tests. This standard establishes that compressive strength is determined by applying a normal force to the surface of the sample and measuring the stress applied when breakage occurs. Compressive strength tests were performed with a Suzpecar machine, model MEM102/50 t. Six samples were broken down for each type of composition. In addition, speed was controlled by the displacement of the top face, which was tensioned at a rate of 0.5 mm/min.

2.5.1. Acid attack test

Resistance to sulfuric acid attack was measured using six samples after they had been cured for 28 days. Three were exposed to air and three were immersed in 1 molar sulfuric acid for 14 days. The acid volume used was 3 times the volume of the samples, all the surfaces were exposed to the acid attack as it can be seen in Figure 2. They were hanging and during the 15 days the total volume of acid was constant, since acid was renewed as water evaporated, keeping the acid volume constant. Samples were removed from their containers and their compressive strengths were measured after immersion (39).

Results are expressed as the ratio between the compressive strength of the mortars immersed in

Figure 2. Samples during de acid test.

acid and that of the mortars exposed to air, as this calculation shows:

$$\text{Compressive strength variation (\%)} = \frac{C_i - C_{air}}{C_{air}} \cdot 100 \quad [5]$$

where C_i (MPa) is Compressive strength of mortars immersed in acid after 14 days and C_{air} (MPa) is the Compressive strength of non-immersed after 14 days.

3. RESULTS

3.1. Characterization of materials

The chemical composition using an X-ray fluorescence spectrometer of all components is shown on Table 3. SiO_2 was the component most present in recycled sand, although standard sand contained a higher proportion of it. CaO, Al_2O_3 and Fe_2O_3 were also among the main components of recycled sand. Given that recycled aggregate results from construction and demolition waste, its composition is similar to that of cement (without considering SiO_2).

The specific gravity of recycled sand is lower than that of standard sand. The specific gravity of recycled aggregate is lower than that of natural aggregates due to the mixture of materials (e.g., Portland cement, concrete, gypsum, bricks) that form CDW (40).

The particle size distribution of standard and recycled sand was measured with a particle size analyzer (Mastersizer 3000, Malvern, UK) and is presented in Figure 3. The cumulative percentage is represented by continuous lines, while dotted lines represent the total percentage.

CDW had smaller particle size than natural river sand. Cement was the component with the smallest particle size, with an particle size interval between 0 and 150 μm. Although the particle size distribution is a key factor on the properties of the mortars, in this study, the different sands have no been subjected to any previous treatment (except the previous sieving at 1.25 mm for both) in order to compare the results as they were received. According to the technical data sheet the composition of GO consists of the following elements: C (49-56%), O (41-50%), S (2-4%), H (0-1%) and N (0-1%).

Fourier-transform infrared spectroscopy (FTIR) measurements were performed on a Nicolet 380 infrared spectrometer (Thermo Electron Corporation, USA). To perform the FTIR, 1 mg paste powder samples were mixed with 100 mg KBr to produce slices. The FTIR spectrum of graphene oxide is shown in Figure 4; the curve exhibits a sizable peak at 3216 cm^{-1} in the high frequency region, which is related to the stretching mode of the O-H bond and reveals the existence of hydroxyl groups in the graphene oxide. The carboxyl group was assigned to the band at 1724 cm^{-1}. The stretching and bending vibration

Table 3. Main chemical components.

Component (%)	Portland cement	Standard sand	Recycled sand
SiO_2	13.83	96.21	52.60
Al_2O_3	3.53	0.76	7.08
Fe_2O_3	2.26	0.22	3.06
MnO	0.06	-	0.05
MgO	0.70	-	1.84
CaO	59.33	0.13	18.50
Na_2O	0.08	0.05	0.71
K_2O	0.48	0.30	1.38
TiO_2	0.19	0.12	0.40
P_2O_5	0.06	0.01	0.09
SO_3	1.68	0.02	0.03
Cl	<0.03	<0.03	<0.03
Loss on ignition	15.50	0.31	12.27
Specific gravity (g/cm^3)	3.18	2.62	1.68

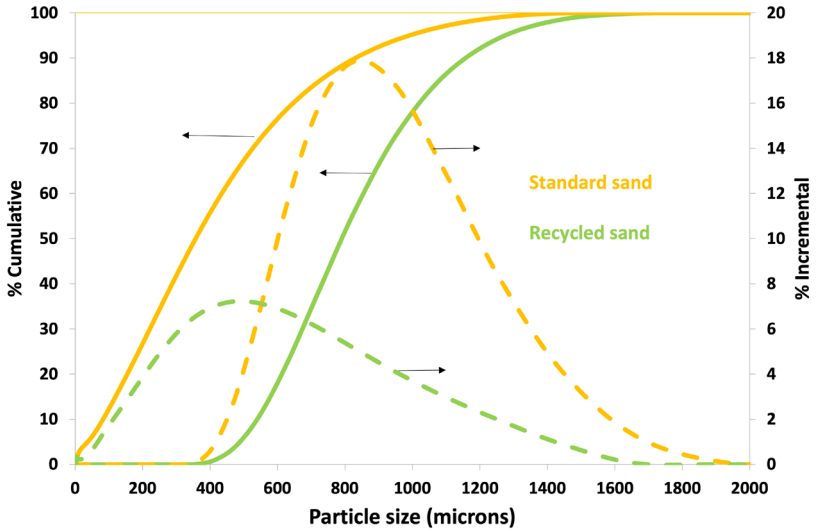

Figure 3. Particle size distribution of standard sand, recycled sand and Portland cement.

of the C=C groups of the water molecules adsorbed on the graphene oxide may have caused the peak at 1610 cm^{-1}. The C-O-H group was responsible for the peak at 1366 cm^{-1}. The peak at 1046 $cm^{-1}$was the vibrational mode of the C-O group, and the peak at 1173 cm^{-1} represented C-O-C stretching.

The time and power of ultrasonication of GO to achieve a good dispersion of GO were very variable in previous studies. In some cases, samples were exposed for 5 minutes (41), while in others they were exposed for about 3 hours (42). For instance, in (21, 28) GO was not even ultrasonicated. Ultrasonication breaks GO sheets, producing smaller platelets. Therefore, the size of GO sheets decreases with increasing time and power. The two types of sand used in this study had a relatively large particle size (between 0.1 and 1 mm), which was expected to mark their mechanical performance (43). Therefore, a moderate sonication process was carried out to adequately determine the particle size of GO and the pore size of the matrix, because smaller pore sizes of GO do not affect the larger pores of the matrix. The GO solution was previously agitated for 24 hours. GO was sonicated for 15 minutes using an ULTRASONS 3000513 device with a power of 150 W to increase the dispersion of graphene oxide nanoparticles in water.

The distribution of graphene oxide is shown in Figure 5. It was measured with a high-definition digital particle size analyzer (Saturn DigiSizer II). Different peaks can be seen in Figure 5 due to the three dimensions of GO (i.e., thickness, width, and length). The two larger peaks – at 2.5 and 4 mm – correspond to the width and length and are quite wide, which means that a high level of dispersion was not reached. The two smaller peaks (at 0.8 and 1.6 mm) correspond to particles of different thicknesses and indicate the low GO-dispersion achieved.

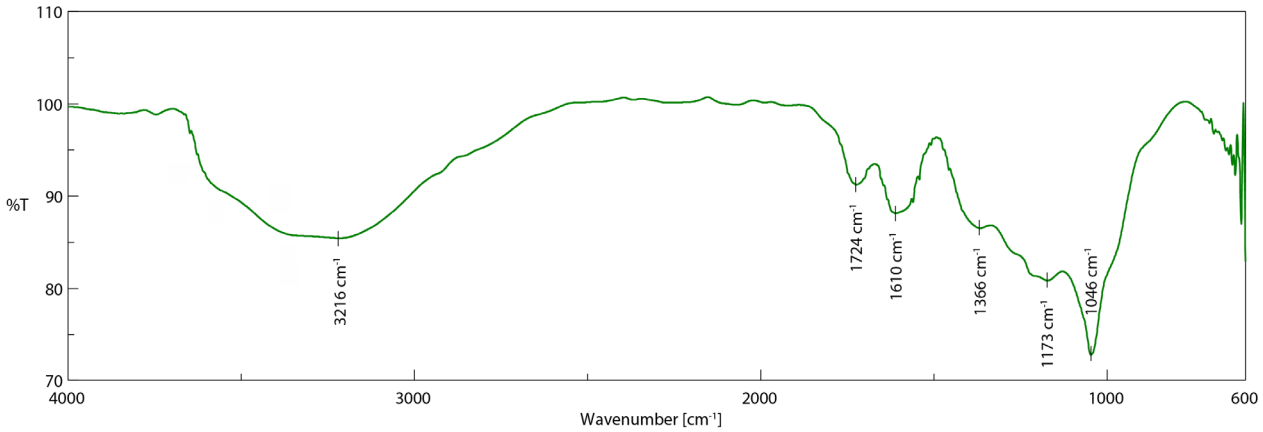

Figure 4. Graphene oxide IR spectrum.

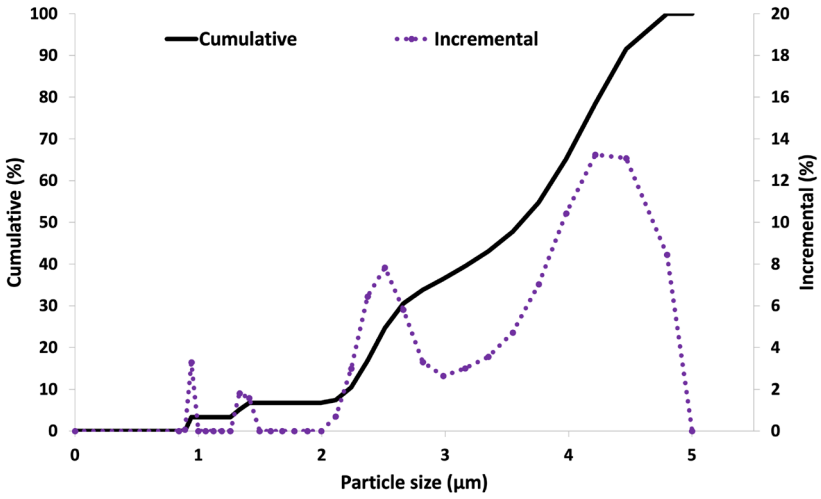

Figure 5. Particle size distribution of graphene oxide.

3.2. Leaching study

Table 4 shows the concentration of leached heavy metals according to EN-12457 (33) of standard sand and recycled sand. The results were also compared to the limits set by European landfill regulations (44), which establish three categories of waste: inert, non-hazardous and hazardous. Recycled waste (and standard sand) can be considered as inert waste because both meet the limits set in the regulations.

Table 4. Leaching results of standard and recycled sand.

	Standard sand (mg/kg)	Recycled sand (mg/kg)	Inert waste (mg/kg)	Non-hazardous waste (mg/kg)	Hazardous waste (mg/kg)	Italian Ministerial Decree 186 (34) (mg/kg)
As	≤0.05	≤0.05	0.5	2	25	0.5
Ba	0.82	0.17	20	100	300	10
Ca	76.62	5989.6	-	-	-	-
Cd	≤0.01	≤0.01	0.04	1	5	0.05
Co	0.01	0.01	-	-	-	2.5
Cr	≤0.02	≤0.02	0.5	10	70	0.5
Cu	≤0.015	≤0.015	2	50	100	0.5
Hg	≤0.005	≤0.005	0.01	0.2	2	0.01
K	5.99	226.32	-	-	-	-
Mg	6.96	2.21	-	-	-	-
Mo	≤0.02	≤0.02	0.5	10	30	-
Na	1.94	230.45	-	-	-	-
Ni	≤0.05	≤0.05	0.4	10	40	0.1
Pb	≤0.015	≤0.015	0.5	10	50	0.5
Sb	≤0.015	≤0.015	0.06	0.7	5	-
Se	≤0.025	≤0.025	0.1	0.5	7	0.1
Sn	≤0.01	≤0.01	-	-	-	-
V	≤0.02	0.29	-	-	-	2.5
Zn	0.67	≤0.02	4	50	200	0.03

In Italy, EN 12457-1 (33) results are used to determine whether waste can be used in construction materials. According to the limits of the Italian Ministerial Decree (34), CDW could be used as they do not exceed any limits, but Standard Sand exceeds the limit set for Zn.

3.3. Physical properties

3.3.1. Density

Figure 6 shows the density of the different compositions with standard sand and CDW waste, with and without the addition of GO. Density is related to two parameters: particle size distribution and the specific gravity of the two types of sands. A higher particle size distribution produces higher porosity between the particles. If the specific gravity is lower, it results in higher porosity inside the particles. SS has a slightly higher particle size and a higher specific density (see Figure 3 and Table 1), so standard sand mortars have a higher density than recycled sand mortars.

Regardless of the material mortars are made of, their density decreases as the water/cement ratio rises. This is because when a high water/cement ratio is used, non-reacted water evaporates during the last period of curing and creates a higher number of pores. When CDW aggregate is used, part of the water is stored inside the CDW aggregate producing a lower density diminution.

As shown by Figure 6, the addition of GO did not affect the mortar density because the amount of GO added was very low. Nevertheless, the effect of GO on the pore size distribution of mortars was very significant (Figure 7). By adding GO, large pores decreased in size and were divided into smaller pores. Between 100 and 1000 µm, the number of large pores decreased, and a larger number of pores between 10 and 100 µm appeared. The peak clearly displaced to finer pores with the addition of GO, and pore volume

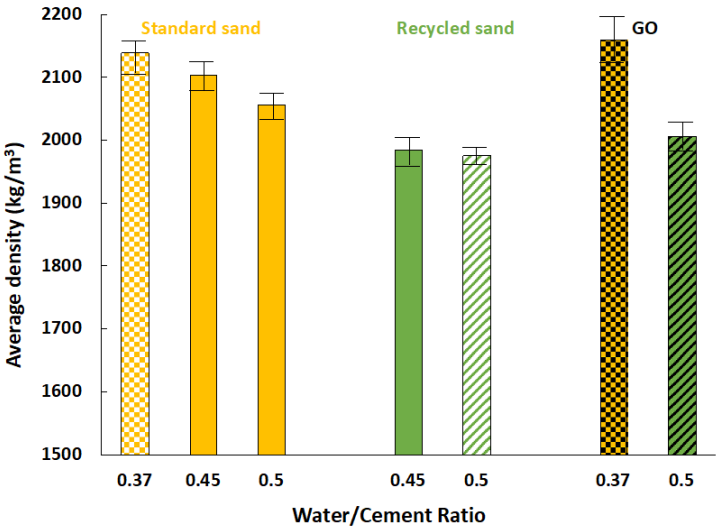

Figure 6. Density of mortars with different fine aggregates and GO addition.

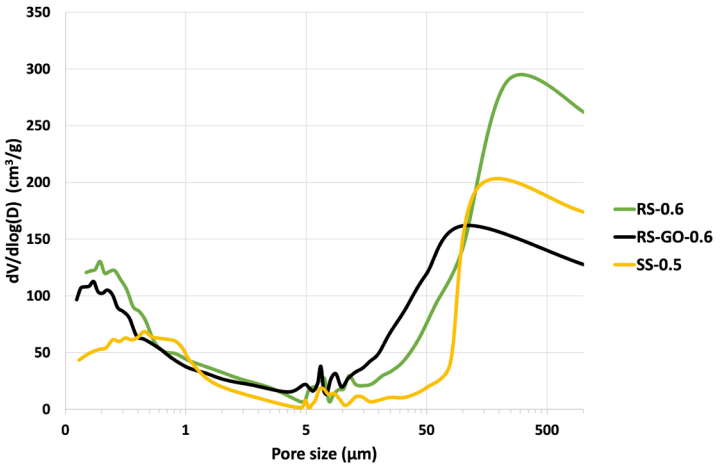

Figure 7. Porosimetry of mortars with CDW and the same water/cement ratio.

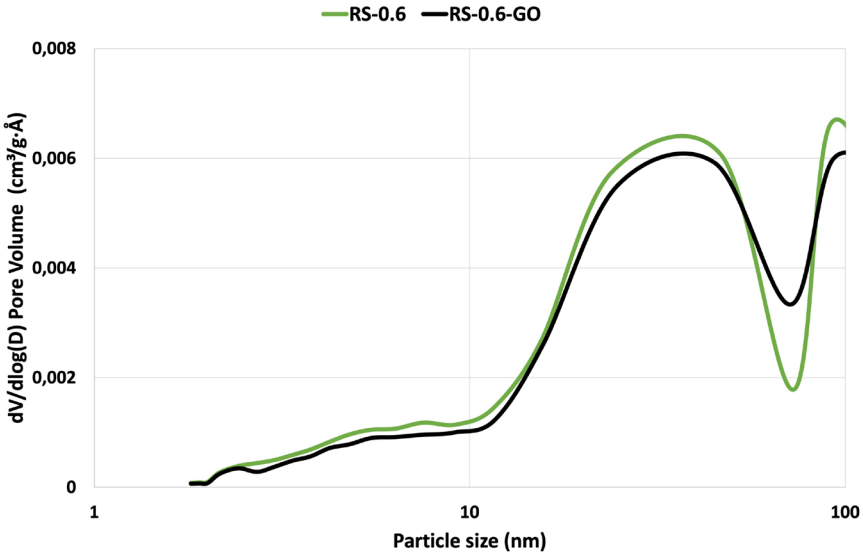

Figure 8. Nanopores of mortars with CDW and the same water/cement ratio.

decreased significantly. The same thing happened to the peak around 0.1 µm: thanks to the addition of GO, the number of pores of that size decreased.

To analyze the influence in pores smaller than 0.1 µm, gas adsorption measurements were performed (Figure 8). As can be seen, there was an increase in the number of nanopores between 60 and 100 nanometers when GO was added. This increase was due to the previous reduction of pores by the addition of 0.1 µm GO. If GO with a low particle size had been used, the largest pores in the mortar would not have undergone any changes.

3.3.2. Humidity, water absorption capacity and porosity.

Table 5 presents other physical properties: humidity content, water absorption capacity and open void porosity.

As mentioned above, when the water/cement ratio is higher, the density is lower because more pores are formed. These properties are inversely related to density, so we expected humidity content, water absorption capacity and open void porosity to be higher when density decreased. When GO was added, density remained almost constant, but pore size decreased, preventing water from entering the sample during these tests.

3.4. Mechanical properties

Figure 9 shows the flexural strength of mortars with different compositions after the 28-day curing period. The strength of all mortars decreased as the amount of water increased. This happened because of the growth in porosity.

There was a considerable difference in the flexural strength values obtained between the two materials.

Table 5. Humidity content, water absorption capacity and open void porosity results.

Mortars	Humidity (%)	Water absorption capacity (%)	Open void porosity (%)
SS- W/PC=0.37	5.6	8.3	17
SS- W/PC=0.45	5.7	10.1	20
SS- W/PC=0.5	5.8	10.8	22
RS- W/PC=0.5	6.9	15.6	26
RS- W/PC=0.6	8.1	15.6	28
GO-SS- W/PC=0.37	4.1	5.4	10
GO-RS- W/PC=0.6	5.1	8.8	14

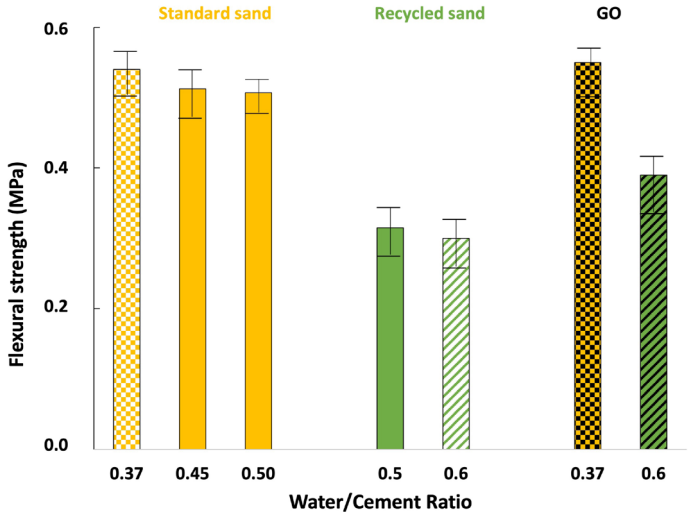

Figure 9. Flexural strength of mortars with different fine aggregates and GO addition.

Standard sand showed better results than CDW with the same water/cement ratio. The addition of GO improved the flexural strength of recycled waste. The improvement was greater for CDW.

The mechanical properties of mortars are very dependent on their microstructure. The corresponding SEM images of the mortars were also examined to determine the link between mechanical strength and microstructure. SEM images of the microstructure of mortars containing recycled aggregate with and without GO are shown in Figure 10. When the mortar did not contain GO, many needle- and bar-like crystals emerged on the fracture surface; they were disorderly stacked cement hydration crystals of ettringite and/or gypsum (Figure 9A). it is not easy to distinguish both. During the initial stage of hydration, ettringite decomposes to produce monosulfate, and at the same time, sulfate ions can be adsorbed in calcium silicate hydrates. Then, at ambient temperature, the sulfate ions adsorbed in calcium silicate hydrates leach out and react with monosulfate to form ettringite (45). Since GO is not easy to found at the presented doses. It has been postulated (46-47) that GO sheets act as 2D platforms to guide the formation of 2D calcium silicate hydrated microplates with a dense nanostructure form a 3D network that can mechanically reinforce the cement paste at the nanoscale. GO regulates the morphology of calcium silicate hydrates and induces the formation of compact, flower-like C–S–H crystals, so flexural strength was greater (24, 48). GO gives a filler effect, supplies more nucleation sites at the time of the hydration process, and regulates the development of cement hydration crystals (49).

Figure 11 shows the effect of water/cement ratio, type of sand and GO addition on compressive strength; its variation was like flexural strength.

According to CEDEX, the Spanish National Public Works Research Centre (8), when 100% fine aggregates are replaced by recycled mortars instead of standard aggregates, compressive strength can de-

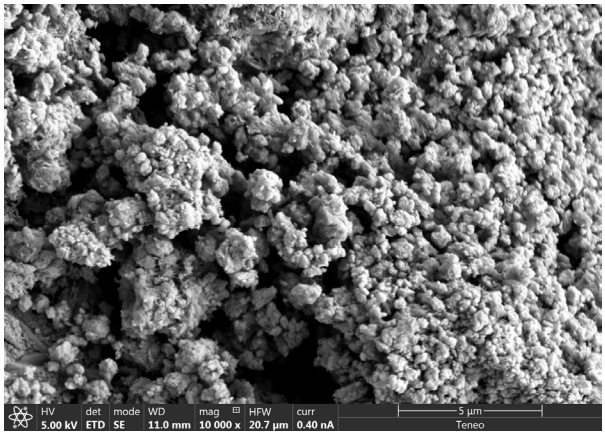

A

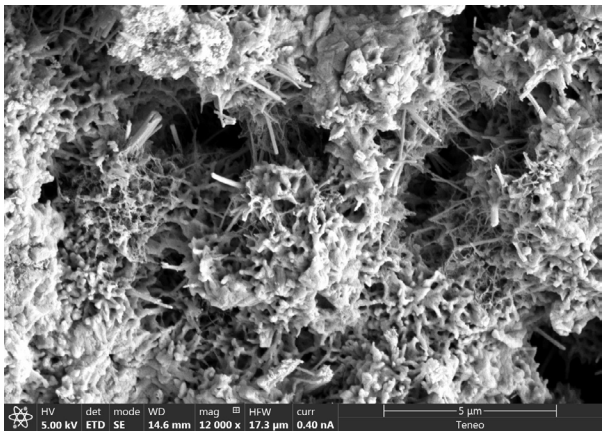

B

Figure 10. SEM images of mortars with recycled aggregates at 28 days and the same water/cement ratio: (A) without GO; (B) with GO.

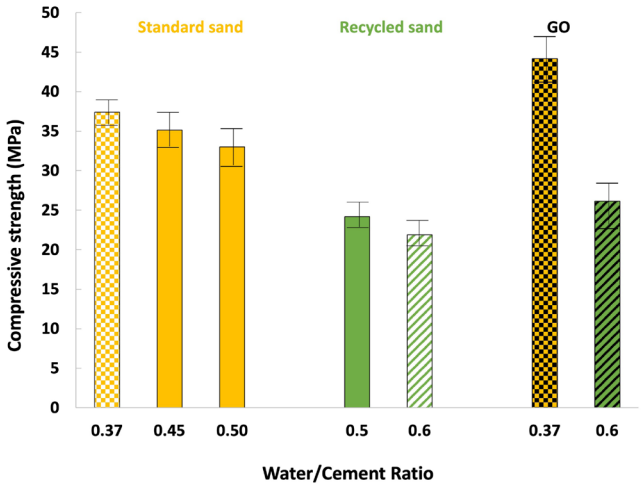

Figure 11. Compressive strength of mortars with different fine aggregates and GO addition.

crease by 33%. In this case, the experiment showed a 36% loss in compressive strength using recycled aggregate.

The addition of GO to standard sand and recycled sand mortars resulted in an improvement of approximately 20% in both samples. The action of GO benefitted from enhanced compressive strength. This material reduced the size of internal pores and reinforced its internal structure, leading to a decrease of large pores and an improvement of compressive strength.

The improvement in compressive strength due to the addition of small amounts of GO has been shown by many studies (27, 48, 49). The introduction of small amounts of GO – as little as 0.0075% by weight – increased compressive strength by 15-33%. The polyhedron-like crystal hydration products formed a compacted structure and had greater compressive strength (Figure 9).

As can be seen in the figure, all mortars exceeded a compressive strength of 20 MPa. Thus, according to the EN 998-2 (50) specifications for masonry mortars, they would be classified as class M20.

3.4.1. Acid attack test

The properties related to CDW durability have been studied previously (51), the foreign agents move through concrete by flowing through the porous system and diffusion and sorption, which introduces corrosion hazards. Figure 12 shows the variation in compressive strength in a mortar after immersion in acid for 14 days, compared to a mortar that was not immersed for the same period.

Acid attack resistance decreases with higher water/cement ratios and with the addition of recycled aggregate because open void porosity increases (see

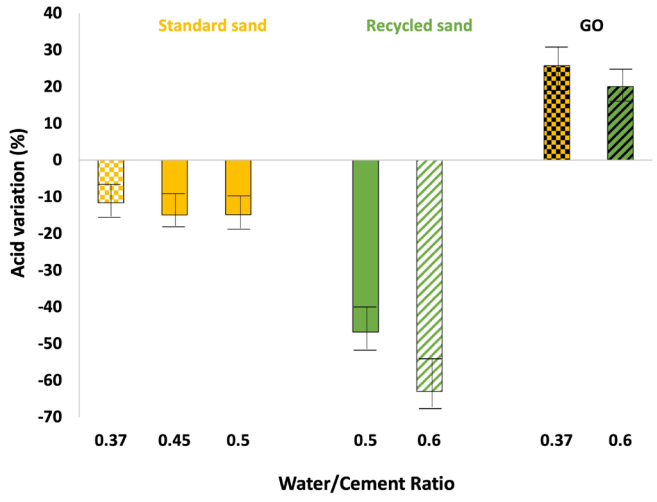

Figure 12. Compressive strength ratio of acid-immersed and non-immersed mortars.

Table 5). Sulphuric acid attacks the matrix, producing gypsum inside the pores, which causes pore spalling and results in worse mechanical properties than cement. As CDW is made up of cement and concrete waste, the reactivity of recycled aggregate increases, decreasing acid resistance; by contrast, standard aggregate is composed mainly of SiO_2, which is not reactive, so only the cement matrix is affected by the acid attack.

Figure 13. Outer appearance of recycled sand mortar after immersion in acid.

Figure 13 shows a mortar made from recycled fine aggregate with a water/cement ratio of 0.6 and added GO after 14 days of immersion and two days of drying. The sample is covered by a white layer due to the formation of $CaSO_4 \cdot H_2O$ in the acid attack.

When GO was added, the pore size distribution was lower, which prevented the entry of water (and acid); only gypsum was formed outside and the interior matrix remained unchanged (see Figure 13).

A recycled sand mortar with a water/cement ratio = 0.6 with GO is presented above (Figure 14. A) after the compression test. The sample had a white layer covering the surface, and the inside of the mortar had the colour of cement, which indicated that the attack was only superficial due to the addition of GO. Figure 14.B shows the standard sand mortar with a water/cement ratio = 0.5 without GO when the acid had penetrated the core of the mortar, after the compression test, although it is not as marked as in the outer zone of both samples. Due to its high-water absorption capacity, the acid was able to penetrate more easily, and gypsum formed on the inside, contributing to the breakdown of the material as a result of spalling.

4. CONCLUSIONS

The following conclusions were drawn from this study:

- The W/C ratio affected all properties. Samples with a lower ratio had better physical and mechanical properties, as their porosity was lower. Recycled aggregates present a higher W/C ratio, due to its lower specific density, which absorb the water during the mixing.
- Mortars made with standard sand had higher density than those made with recycled sand. Density depends on particle size distribution and specific gravity. According to the compressive strength. Both mortars with two aggregates can be classified as M20, although the particle size of the aggregates is very important factor.
- The addition of GO improved the properties of mortars with both sands, as graphene oxide reduces the macro and micropores, increasing the nano-pores, obtaining similar total porosities, but increasing the mechanical properties because the nano-pores have no influence in the properties.

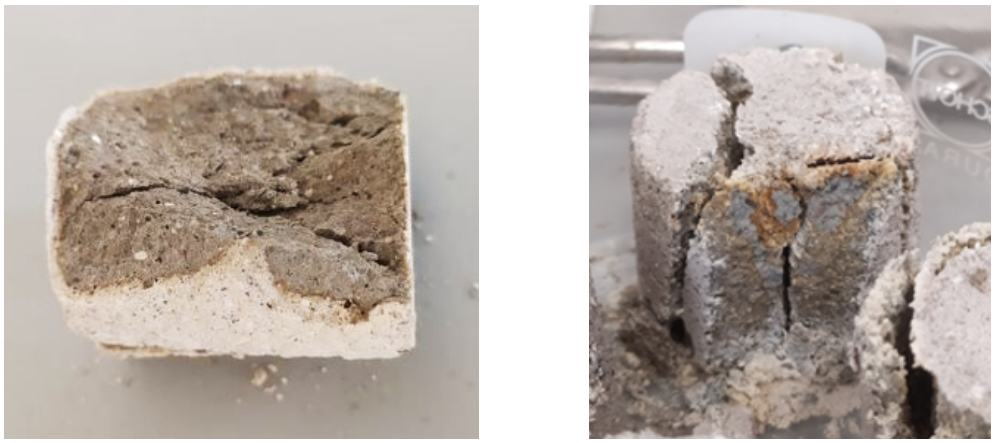

A **B**

Figure 14. A) Mortar with recycled aggregate and water/cement ratio = 0.6 with GO and B) mortar with standard sand and water/cement ratio = 0.5 without GO.

- Graphene oxide acts as a nucleation site for the formation of hydration products during the cement hydration process which accelerates the early-stage hydration reactions, leading to the formation of denser cementitious products which derive into higher compressive and flexural strength.
- Regarding the acid attack, as recycled sand mortars are more porous, compressive strength decreased more in the samples containing recycled sand than in those containing standard sand. Although the attack was carried out outside of the samples, the addition of GO in mortars made with both types of sand prevented the entry of the acid solution inside and showed a positive compressive strength after the acid immersion.
- The addition of GO in mortars made with both types of sand prevented the entry of the acid solution inside and showed a positive compressive strength in acid immersion.
- Standard sand typically has well-rounded particles with a consistent size distribution. This allows for better particle packing and interlocking, resulting in a denser mortar matrix. In contrast, waste sand has irregular particle shapes, impurities, porosity and varying size distributions, leading to less efficient packing and reduced mortar density which conducts to lower mechanical properties and durability.

Although the flexural and compressive results of recycled sand were lower than those of standard sand, they all satisfied the standard and the strengths obtained were sufficient for compliance with EN standard on use in construction sites as masonry mortars.

ACKNOWLEDGEMENTS:

The authors would like to acknowledge the financial support provided to this study by the Regional Government of Andalusia, Spain (Junta de Andalucía - Consejería de Economía y Conocimiento) under projects US-1266248 and P18-RT-1485.

AUTHOR CONTRIBUTIONS:

Conceptualization: C. Leiva. Data curation: Y. Luna-Galiano. Formal analysis: H. Cifuentes. Funding acquisition: P. Ariza. Investigation: C. Chacón Bonet. Methodology: J.D. Rios. Project administration: P. Ariza. Resources: Y. Luna-Galiano. Supervision: C. Leiva. Validation: P. Ariza. Visualization: H. Cifuentes. Writing, original draft: C. Chacón-Bonet. Writing, review & editing: J.D. Rios.

REFERENCES

1. Luo, J.; Chen, S.; Li, Q.; Liu, C.; Gao, S.; Zhang, J.; Guo, J. (2019) Influence of graphene oxide on the mechanical properties, fracture toughness, and microhardness of recycled concrete. *Nanomat.* 9 [3], 325. https://doi.org/10.3390/nano9030325.
2. De Oliveira Andrade, J.J.; Possan, E.; Squiavon, J.Z.; Ortolan, T.L.P. (2018) Evaluation of mechanical properties and carbonation of mortars produced with construction and demolition waste. C*onstr. Build. Mater.* 161, 70–83. https://doi.org/10.1016/J.CONBUILDMAT.2017.11.089.
3. Porras-Amores, C., Martin Garcia, P., Villoria Sáez, P., del Rio Merino, M.; Vitielo, V. (2021) Assessing the energy efficiency potential of recycled materials with construction and demolition waste: a spanish case study. *Appl. Sci.* 11 [17], 7809. https://doi.org/10.3390/app11177809.
4. Directive (EU) 2018/851 of the European Parliament and the Council Amending Directive 2008/98/EC on waste. Off J. Eur. Union n.d.
5. Directive 2008/98/EC of the European Parliament and the Council on Waste. Off J. Eur. Union n.d.
6. European Commission. Protocol on the management of construction and demolition waste in the EU, September 2016. n.d.
7. Junta de Andalucía. Integrated waste plan for Andalusia. Towards a circular economy in the 2030 Horizon., PIRE 2030. 5 April 2021 n.d. Retrieved from https://www.juntadeandalucia.es/medioambiente/portal/documents/20151/26992369/2021_10_19_PIRec_completo5.pdf/6c1a646a-c293-79ca-c201-a9f3386b86ce?t=1634807843024.
8. CEDEX. Construction and demolition waste. Waste usable in construction. November 2014. Retrieved from https://www.cedexmateriales.es/upload/docs/es_RESIDUOSDECONSTRUCCIONYDEMOLICIONNOV2014.pdf.
9. Kabirifar, K.; Mojtahedi, M.; Wang, C.; Tam, V.W.Y. (2020) Construction and demolition waste management contributing factors coupled with reduce, reuse, and recycle strategies for effective waste management: A review. *J. Clean. Prod.* 263, 121265. https://doi.org/10.1016/J.JCLEPRO.2020.121265.
10. Bao, Z.; Lu, W. (2020) Developing efficient circularity for construction and demolition waste management in fast emerging economies: Lessons learned from Shenzhen, China. S*ci. Total Environ*. 724, 138264. https://doi.org/10.1016/J.SCITOTENV.2020.138264.
11. CEDEX. Recycled aggregate from concrete. Retrieved from https://www.cedexmateriales.es/catalogo-de-residuos/34/reciclado-de-pavimentos-de-hormigon/
12. Zhou, Y.; Gong, G.; Huang, Y.; Chen, C.; Huang, D.; Chen, Z.; Guo, M. (2021) Feasibility of incorporating recycled fine aggregate in high performance green lightweight engineered cementitious composites. *J. Clean. Prod.* 280 [2], 124445. https://doi.org/10.1016/J.JCLEPRO.2020.124445.
13. Long, W.J.; Zheng, D., Duan, H.; Han, N.; Xing, F. (2018) Performance enhancement and environmental impact of cement composites containing graphene oxide with recycled fine aggregates. *J. Clean. Prod.* 194, 193–202. https://doi.org/10.1016/J.JCLEPRO.2018.05.108.
14. Shi, C.; Li, Y.; Zhang, J.; Li, W.; Chong, L.; Xie, Z. (2016) Performance enhancement of recycled concrete aggregate – A review. *J. Clean. Prod.* 112 [1], 466–472. https://doi.org/10.1016/J.JCLEPRO.2015.08.057.
15. EN 13139. (2003) Aggregates for mortar, European Committee for Standardization.
16. prEN 12620. (2002) Aggregates for concrete. European Committee for Standardization.
17. EN 13055-1. (2003) Lightweight aggregates - Part 1: Lightweight aggregates for concrete, mortar and grout. European Committee for Standardization.
18. prEN 13242. (2017) Aggregates for bituminous mixtures and surface treatments for roads, airfields and other trafficked areas. European Committee for Standardization.
19. Tobón, J.I.; Payá, J.; Restrepo, O.J. (2015) Study of durability of Portland cement mortars blended with silica nanoparticles. *Constr. Build. Mater.* 80, 92–97. https://doi.org/10.1016/J.CONBUILDMAT.2014.12.074.
20. Liu, J., Li, Q.; Xu, S. (2015) Influence of nanoparticles on fluidity and mechanical properties of cement mortar. *Constr. Build. Mater.* 101 [1], 892–901. https://doi.org/10.1016/J.CONBUILDMAT.2015.10.149.
21. Mohammed, A.; Sanjayan, J.G., Duan, W.H.; Nazari, A. (2015) Incorporating graphene oxide in cement composites: A study of transport properties. *Constr. Build. Mater.* 84, 341–347. https://doi.org/10.1016/J.CONBUILDMAT.2015.01.083.

22. Zhao, L.; Guo, X.; Song, L.; Song, Y.; Dai, G.; Liu, J. (2020) An intensive review on the role of graphene oxide in cement-based materials. *Constr. Build. Mater.* 241, 117939. https://doi.org/10.1016/J.CONBUILDMAT.2019.117939.
23. Wang, W.; Jian-Chen, S.; Sagoe-Crentsil, K.; Duan, W. (2022) Graphene oxide-reinforced thin shells for high-performance, lightweight cement composites. *Composites Part B: Engineering* 235, 109796. https://doi.org/10.1016/j.compositesb.2022.109796.
24. Lv, S.; Ma, Y.; Qiu, C.; Sun, T.; Liu, J.; Zhou, Q. (2013) Effect of graphene oxide nanosheets of microstructure and mechanical properties of cement composites. *Constr. Build. Mater.* 49, 121–127. https://doi.org/10.1016/j.conbuildmat.2013.08.022.
25. Lv, S.; Ma, Y.; Qiu, C.; Zhou, Q. (2013) Regulation of GO on cement hydration crystals and its toughening effect. *Mag. Concr. Res*. 65 [20], 1246–1254. https://doi.org/10.1680/macr.13.00190.
26. Lv, S.; Liu, J.; Sun, T.; Ma, Y.; Zhou, Q. (2014) Effect of GO nanosheets on shapes of cement hydration crystals and their formation process. *Constr. Build. Mater.* 64, 231–239. https://doi.org/10.1016/J.CONBUILDMAT.2014.04.061.
27. Li, W.; Li, X.; Chen, S.J.; Liu, Y.M.; Duan, W.H.; Shah, S.P. (2017) Effects of graphene oxide on early-age hydration and electrical resistivity of Portland cement paste. *Constr. Build. Mater.* 136, 506–514. https://doi.org/10.1016/j.conbuildmat.2017.01.066.
28. Li, X.; Wang, L.; Liu, Y.; Li, W.; Dong, B.; Duan, W.H. (2018) Dispersion of graphene oxide agglomerates in cement paste and its effects on electrical resistivity and flexural strength. *Cem. Concr. Compos*. 92, 145–154. https://doi.org/10.1016/j.cemconcomp.2018.06.008.
29. Li, X.; Li, C.; Liu, Y.; Chen, S.J.; Wang, C.M.; Sanjayan, J.G.; Duan, W.H. (2018) Improvement of mechanical properties by incorporating graphene oxide into cement mortar. *Mech. Adv. Mater. Struct.* 25 [15-16], 1313–1322. https://doi.org/10.1080/15376494.2016.1218226.
30. Peng, H.; Ge, Y.; Cai, C.S.; Zhang, Y.; Liu, Z. (2019) Mechanical properties and microstructure of graphene oxide cement-based composites. *Constr. Build. Mater.* 194, 102–109. https://doi.org/10.1016/J.CONBUILDMAT.2018.10.234.
31. EN 197-1. (2011) Cement - Part 1: Composition, specifications and conformity criteria for common cements, European Committee for Standardization.
32. Leiva, C.; Solís-Guzmán, J.; Marrero, M.; García-Arenas, C. (2013) Recycled blocks with improved sound and fire insulation containing construction and demolition waste. *Waste Manag*. 33 [3], 663–671. https://doi.org/10.1016/j.wasman.2012.06.011.
33. EN 12457-4. (2003) Characterisation of waste - Leaching - Compliance test for leaching of granular waste materials and sludges. Part 4: One stage batch test at a liquid to solid ratio of 10 l/kg for materials with particle size below 10 mm (without or with size reduction), European Committee for Standardization.
34. IMD 186. (2006) Individuazione dei rifiuti non pericolosi sottoposti alle procedure semplificate di recupero ai sensi degli articoli 31 e 33 del decreto legislativo 05/02/1997. Gazzetta Ufficiale n. 115.
35. EN 12859. (2012) Gypsum blocks. Definitions, requirements and test methods. European Committee for Standardization. Brussels, Belgium.
36. ASTM C642-21. (2021) Standard test method for density, absorption, and voids in hardened concrete. ASTM International (ASTM).
37. ASTM C348. (2021) Standard test method for flexural strength of hydraulic-cement mortars, ASTM International (ASTM).
38. EN 196-1. (2018) Methods of testing cement - Part 1: Determination of strength, European Committee for Standardization.
39. Cerulli, T.; Pistolesi, C.; Maltese, C.; Salvioni, D. (2003) Durability of traditional plasters with respect to blast furnace slag-based plaster. *Cem. Concr. Res.* 33 [9], 1375–1383. https://doi.org/10.1016/S0008-8846(03)00072-3.
40. Arenas, C.; Luna-Galiano, Y.; Leiva, C.; Vilches, L.F.; Arroyo, F.; Villegas, R.; Fernandez-Pereira, C. (2017) Development of a fly ash-based geopolymeric concrete with construction and demolition wastes as aggregates in acoustic barriers. *Constr. Build. Mater.* 134, 433–442. https://doi.org/10.1016/J.CONBUILDMAT.2016.12.119.
41. Li, X.; Korayem, A.H.; Li, C.; Liu, Y.; He, H.; Sanjayan, J.G.; Duan, W.H. (2016) Incorporation of graphene oxide and silica fume into cement paste: A study of dispersion and compressive strength. *Constr. Build. Mater.* 123, 327–335. https://doi.org/10.1016/J.CONBUILDMAT.2016.07.022.
42. Horszczaruk, E.; Mijowska, E., Kalenczuk, R.J.; Aleksandrzak, M.; Mijowska, S. (2015) Nanocomposite of cement/graphene oxide – Impact on hydration kinetics and Young's modulus. C*onstr. Build. Mater.* 78, 234–242. https://doi.org/10.1016/J.CONBUILDMAT.2014.12.009.
43. Ríos, J.D.; Leiva, C.; Ariza, M.P.; Seitl, S.; Cifuentes, H. (2019) Analysis of the tensile fracture properties of ultra-high-strength fiber-reinforced concrete with different types of steel fibers by X-ray tomography. *Mater. Des.* 165, 107582. https://doi.org/10.1016/j.matdes.2019.107582.
44. Council Directive 1999/31/EC of 26 April (1999) On the landfill of waste. Official Journal L. 182, 16/07/1999 P. 0001 – 0019. European Commission (1999) http://data.europa.eu/eli/dir/1999/31/oj.
45. Ando, Y.; Shinichi, H.; Katayama, T.; Torii, K. (2022) Microscopic observations of sites and forms of ettringite in the microstructure of deteriorated concrete. *Mater. Construcc.* 72 (346), e283. https://doi.org/10.3989/mc.2022.15521.
46. Basquiroto de Souza, F.; Shamsaei, E.; Sagoe-Crentsil, K.; Duan, W. (2022) Proposed mechanism for the enhanced microstructure of graphene oxide–Portland cement composites. *J. Build. Eng.* 54, 104604. https://doi.org/10.1016/j.jobe.2022.104604.
47. Sharma, S.; Kothiyal, N.C. (2015) Influence of graphene oxide as dispersed phase in cement mortar matrix in defining the crystal patterns of cement hydrates and its effect on mechanical, microstructural and crystallization properties. *RSC Adv.* 65, 52642-52657. http://doi.org/10.1039/C5RA08078A.
48. Long, W.J.; Wei, J.J.; Xing, F.; Khayat, K.H. (2018) Enhanced dynamic mechanical properties of cement paste modified with graphene oxide nanosheets and its reinforcing mechanism. *Cem. Concr. Compos*. 93, 127–39. https://doi.org/10.1016/J.CEMCONCOMP.2018.07.001.
49. Wang, M.; Wang, R.; Yao, H.; Farhan, S.; Zheng, S.; Du, C. (2016) Study on the three dimensional mechanism of graphene oxide nanosheets modified cement. *Constr. Build. Mater.* 126, 730–739. https://doi.org/10.1016/j.conbuildmat.2016.09.092.
50. EN 998-2. (2018) Specification for mortar for masonry - Part 2: Masonry mortar. European Committee for Standardization.
51. Gómez-Cano, D.; Arias-Jaramillo, Y.P.; Bernal-Correa, R.; Tobón, J.I. (2023) Effect of enhancement treatments applied to recycled concrete aggregates on concrete durability: A review. *Mater. Construcc.* 73 [349], e308. https://doi.org/10.3989/mc.2023.296522.